The detectability of free-phase migrating CO2

Available online at www.sciencedirect.com

ScienceDirect

Energy Procedia 63 (2014) 4449 – 4458

Energy Procedia

GHGT-12

The detectability of free-phase migrating CO_2: A rock physics and seismic modelling feasibility study

Rami Eid[a], Anton Ziolkowski[a], Mark Naylor[a], Gillian Pickup[b]

[a]*Universityof Edinburgh, Edinburgh, EH9 3FE, United Kingdom*
[b]*Heriot-Watt University, Edinburgh, EH14 4AS, United Kingdom*

Abstract

Subsurface monitoring is essential for the successful implementation and public acceptance of CO_2 storage. Injected CO_2 will need to be monitored to verify the successful containment within its intended formation, and to ensure no loss of containment within the storage complex. The ability for seismic techniques to monitor structurally trapped CO_2 has been successfully demonstrated due to the changes in the acoustic properties of the reservoir produced by the displacement of brine by less dense and more compressible CO_2. However, the ability for seismic methods to detect free-phase migrating CO_2 is still moderately understood. In order to assess the feasibility for seismic monitoring of a migrating front, we estimate the time-lapse signal over a theoretical, clean, homogeneous sandstone reservoir through the application of a three-stage model-driven workflow consisting of fluid-flow, rock physics and seismic forward modelling. To capture the range of responses which could be encountered, two end-member fluid distribution models were used: uniform saturation and the modified patchy saturation model. Analysis of the time-lapse survey highlights the importance of determining and understanding the fluid distribution model impacting the range of velocities prior to generating and interpreting the seismic response. This change in velocity is shown to be directly related to the volume of CO_2 occupying the pore-space of a migrating plume front. This highlights the fact that the detectability of a migrating front is a site specific issue which not only depends on the geophysical parameters of the seismic survey but also on the geological variations and spatial distribution in the reservoir.

Peer-review under responsibility of the Organizing Committee of GHGT-12

Keywords: CCS; monitoring; migration; leakage; time-lapse; seismic modelling; rock physics, patchy saturation

*Corresponding author. Tel.: +44(0)-758-276-0792; Fax: +44(0)-131-668-3184
Email address: rami.eid@ed.ac.uk

Peer-review under responsibility of the Organizing Committee of GHGT-12
doi:10.1016/j.egypro.2014.11.480

1. Introduction

The monitorability of CO_2 storage sites is a site-specific issue which involves the monitoring, measurement and verification of injected CO_2 in the subsurface. This is done to demonstrate containment within the intended formation, and importantly, identify and quantity any movement of CO_2 from the primary storage reservoir.

It is favourable that CO_2 injection occurs within a storage complex with two reservoir-seal pairs, representative of a primary and secondary storage site. As defined by the EU CCS directive [1], a storage complex includes the storage site and surrounding geological domains impacting on the overall storage integrity and security of the project. Should a loss of containment within the primary reservoir occur, movement of CO_2 from the primary to secondary reservoir can be expected. This is termed migration. The ability to detect CO_2 migration is seen as critical when demonstrating containment, as the detection of movement from the primary to a secondary storage site could provide operators with an early warning system should a loss of containment occur.

The ability for seismic techniques to monitor structurally trapped CO_2 has been successfully demonstrated at storage sites such as Sleipner [2] and Weyburn [3] due to the changes in the acoustic properties of the reservoir produced by the displacement of brine by less dense and more compressible CO_2 [4]. However, the ability for seismic methods to detect a migrating plume front, often associated with lower CO_2 saturations, is still moderately understood. The process of CO_2 injection disrupts the equilibrium of the reservoir, resulting in multi-phase fluid distributions of different compressibilities within a pore space. As the seismic response depends on both the fluid type and distribution, end-member fluid distribution models are required to predict the possible range of velocities impacting the seismic responses [5-7].

To simulate a loss of containment, and investigate the range of surface seismic responses due to CO_2 migration, we estimate the time-lapse signal over a theoretical, clean, homogeneous sandstone reservoir through the application of a three-stage model-driven workflow consisting of fluid-flow, rock physics and seismic forward modelling. To capture the range of responses which could be encountered, two end-member fluid distribution models are used: the uniform saturation model, and the modified patchy saturation model. Analysis of the time-lapse surveys will provide an understanding as to the potential for surface seismic techniques to detect a loss of containment. This could provide operators with an early warning system, allowing for remediation activities to be undertaken such that the probability of a leak outside the storage complex is negligible.

2. Reservoir model

A three-dimensional theoretical model representative of a sandstone reservoir separated by an intraformational seal with a zone of weakness was built specifically for this study. The model is an adaptation of the leakage model built by Class et al., [8] as part of a benchmark study on problems related to CO_2 storage.

The geological model consists of four layers representing a low angle dome. The model covers an area of 1000m by 500m, with a vertical cell-size resolution of 20m. The top of the model is at 1000m depth and reaches a total depth of 2150m (Fig. 1). The surfaces represent an impermeable seal, top secondary reservoir, intraformational seal, top primary reservoir and basement. Both reservoirs are 400m thick with a 300m thick intraformational seal. The reservoir consists of a clean, homogeneous sandstone with a decreasing porosity profile with depth. Vertical permeability is assumed to be one tenth of the horizontal permeability. Reservoir conditions include a pressure gradient of 10.5 MPa/km and temperature gradient 30°C/km.

3. Numerical modelling: simulating CO_2 migration

Permedia's black oil simulator [9] was used to simulate a loss of containment. This is modelled as a migrating front of CO_2 moving away from the primary reservoir, which, upon reaching a zone of weakness, continues vertically towards a shallower, secondary reservoir. CO_2 is injected at a constant rate of 0.1 MT per year for 10 years over a 50m perforation interval at 2000m. The injection well is situated at the centre of the domain, 250m away from the leakage pathway. The relative permeability and capillary pressure (P_c) curves used to model drainage and imbibition for CO_2 and brine were obtained from experiments performed on the relatively clean, high

porosity Cardium Sandstone [10].

A snapshot of the moment an initial loss of containment occurs is shown in Fig. 2. The simulation shows vertical migration through the zone of weakness and into the secondary storage reservoir. The migrating CO_2 front is shown to consist of very low saturations, ranging from 1-7% with an average of 2.5% (Fig. 2c). Lower saturations such as these play a key role as to whether the change in seismic velocity is great enough to result in a detectable change. Saturations in this range, when modelling buoyancy-dominated CO_2 flow in the reservoir and the effects of capillary pressure and heterogeneity, have been published in papers such as Bryant et al., [11], Silin et al., [12] and Saadatpoor et al., [13]. The structurally trapped CO_2 spans roughly 650m, while the radius of the migrating front is simulated at 30m.

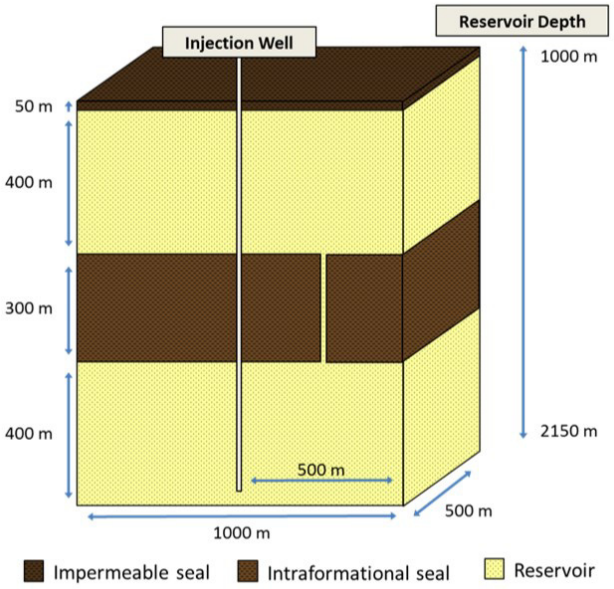

Fig. 1. Reservoir model of a clean homogeneous sandstone reservoir separated by an intraformational seal with a zone of weakness.

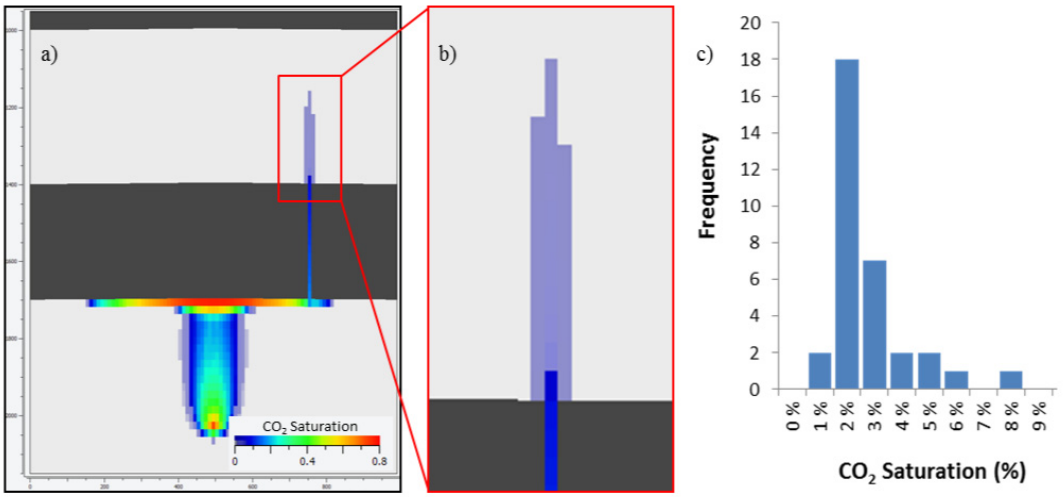

Fig. 2. a) Snapshot from the simulation showing an initial loss of containment, with the migrating plume front highlighted and enlarged (b). c) Histogram showing the range in saturations for the migrating plume front.

4. Rock physics modelling

To predict the change in elastic properties resulting from the migrating front we employ the Gassmann fluid substitution workflow [14]. Gassmann's equation relates the bulk modulus of saturated rocks (K_{sat}) to their porosity (φ), pore-fluid bulk modulus (K_{fl}), matrix bulk modulus (K_m), and dry frame bulk modulus (K_{dry}). Several assumptions limit the applicability of Gassmann's equation. These have been thoroughly discussed by Berryman [17], Smith et al., [14], Han and Batzle [18], and Adam et al., [19]. The main assumption of interest is that the application of Gassmann's equation assumes immiscible and homogeneously distributed phases throughout the pore space (uniform fluid saturation). These assumptions are expected when dealing with systems which have come to equilibrium over long geological timescales; however, during drilling, production, or in this scenario, the migration of CO_2, the distribution of phases may be disturbed. When the migrating CO_2 front is spatially heterogeneous, two pore-fluid distribution end-member ranges are encountered: homogeneous, uniform fluid saturation, and heterogeneous, patchy fluid saturation. As patchy saturation assumes CO_2 saturations from 0-100%, the equation is modified to take into account irreducible water saturation and residual saturation (modified-patchy saturation). Understanding the saturation scales which could be encountered, therefore affecting the changing velocity due to CO_2 migration, is critical when assessing detectability.

4.1. Sensitivity of seismic response to CO_2 fluid distribution model

Fig. 3 shows the expected range in values for P-wave velocity (V_p) predicted using the end-member saturation models used to calculate the fluid bulk modulus (K_{fl}) in Gassmann's equation. The results show that the change in Vp, as a function of CO_2 saturation, is heavily dependent on the saturation model used to calculate the elastic properties. The uniform saturation model predicts a rapid change in Vp as CO_2 saturation increases from 0 to ~20% (a change of ~13%), while showing minimal to no change at higher saturations. However, patchy and modified patchy models predict a linear Vp-saturation relationship showing a gradual change in velocity with increasing saturation. The large range of possibilities highlights the importance of determining the fluid distribution model (uniform/patchy) and therefore applying the most appropriate model for predicting the fluid bulk modulus prior to generating and interpreting the seismic response. Although the uniform and patchy curves represent the upper and lower bounds of fluid bulk modulus for a given saturation, it should be noted that the velocity can be anywhere in between, determined by the permeability, fluid viscosity, and most importantly the size of the migrating front [6, 7, 22].

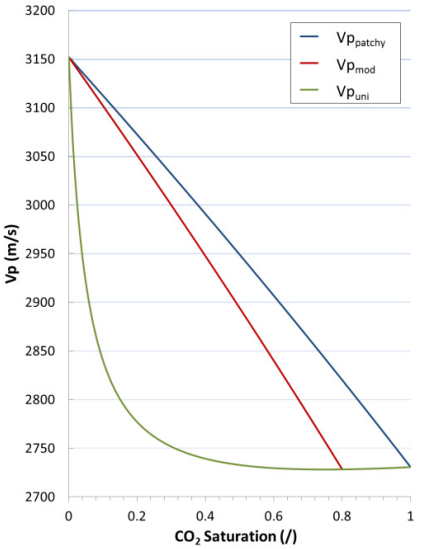

Fig. 3. P-wave velocity (Vp) as a function of CO_2 saturation calculated using: Uniform saturation model (Vp_{uni}), Patchy model, (Vp_{patchy}), and the modified-patchy saturation model assuming an irreducible water saturation of 20% (Vp_{mod}).

When determining the corresponding elastic properties, we assumed both a uniform and modified-patchy saturation. We calculate velocity for each end-member in order to understand the expected ranges which could be encountered when assessing the overall ability to detect a loss of containment. This is done as the calculated velocity is not exact and can be anywhere in between, as both end-member models represent the upper and lower bounds of velocity.

Fig. 4 represents the calculated velocity models assuming both uniform and modified-patchy saturation models during the first instance of a loss of containment. Analysis of the difference between baseline velocity and the velocity at the breach clearly highlights the differences between the two. Velocity calculated using the uniform saturation model clearly shows the outline of the plume, however proves difficult to distinguish features within the plume itself, such as the injection interval or gradational changes in saturation at the structurally trapped region. This is due to the large change in velocity at low CO_2 saturations, and hardly any change thereafter. Velocity calculated using the patchy saturation model clearly distinguishes features in the plume body, as well as the structurally trapped region due to the linear change in velocity with increasing saturation. When focusing on the migrating CO_2 front, it is clear that there is increased potential in detecting the plume front when assuming a uniform saturation model as opposed to patchy saturation, mainly due to the large change in velocity at low saturations. At the migrating front a change in velocity to the baseline is shown to be in the range of -200 to -50 m/s. If assuming that the velocity follows a modified-patchy saturation model, a change of only -50m/s can be expected, which could be difficult to interpret with respect to the baseline.

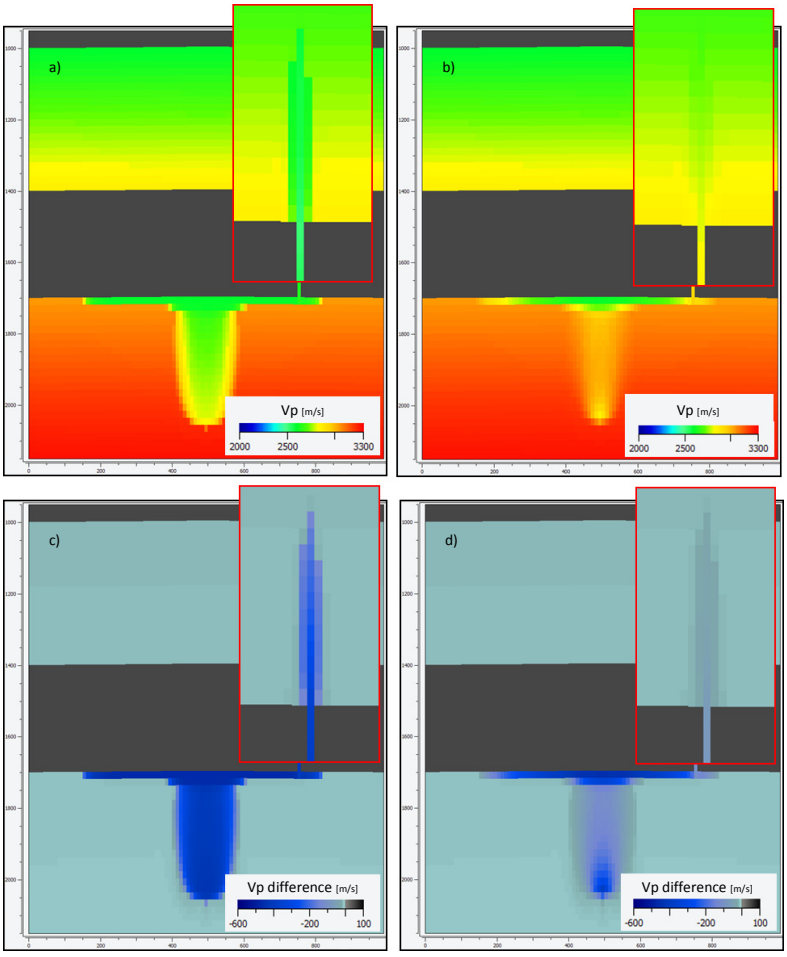

Fig. 4 Vp predicted using Uniform (a) and Modified-patchy saturation (b). The difference in Vp with the baseline assuming uniform saturation (c) and a modified-patchy saturation (d). The migrating front, representing the loss of containment, is highlighted and enlarged in the red box.

5. Seismic forward modelling

In order to assess the potential for seismic monitoring techniques to detect an initial loss of containment, the rock physics modelling results were incorporated into 2D elastic finite-difference wave propagation modelling. Using Nucleus+, we simulated the acquisition of a single line towed streamer survey based on acquisition parameters similar to real time-lapse data (Table 1). In order to get full coverage across the area of interest, the velocity model was extended at both ends by 1km. The modelling was performed on seismic data before and after CO_2 injection, for both uniform and modified-patchy saturation cases. Once acquired, each survey was processed, stacked and depth-migrated using the baseline velocity model.

Table 1.Seismic modelling acquisition parameters.

Acquisition parameters	
Receiver spacing	12.5 m
Source spacing	25 m
Cable length	3000 m
Number of receivers	240
Number of shots	124

The depth-migrated seismic section for the baseline model (pre-injection) is shown below in Fig. 5. The amplitude changes clearly represent the changing lithology within the model. The reflection at 1050m represents the topmost impermeable seal, overlaying the secondary reservoir within the storage complex. The next strong reflector, at 1450m is the top of the 300m thick intraformational seal separating the primary reservoir. The 20m thick zone of weakness, encouraging the migration of CO_2 from the primary to secondary reservoir, is not resolved.

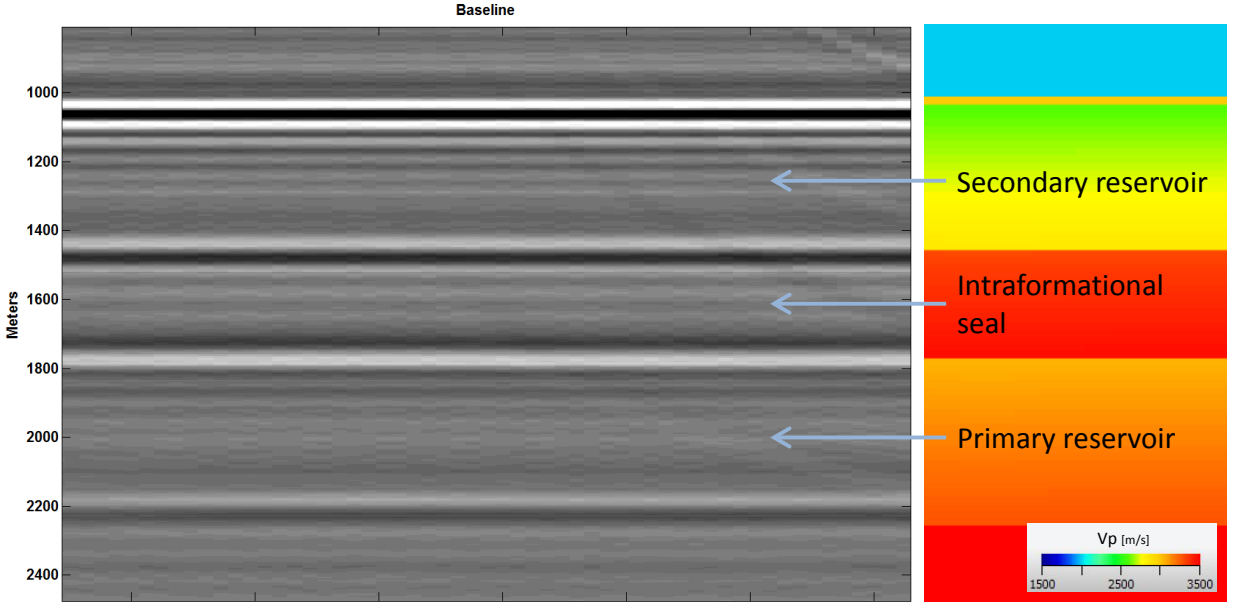

Fig. 5. Depth migrated seismic section of the baseline model, with velocity model highlighting the different layers evident on the seismic section.

5.1. Qualitative observations

As can be expected from seismic modelling, the introduction of CO_2 into the primary reservoir has an increased effect on reflectivity, illustrated in Fig. 6. The accumulated plume, represented by the high amplitude reflection is clearly visible in both models at a depth of roughly 1780m. The plume accumulation is underlain by a prominent velocity pushdown caused by the seismic waves travelling slower through CO_2-saturated rock than through the virgin reservoir. Although not as pronounced in the patchy model, this can be seen at roughly 2200m. No obvious change in amplitude is evident above the intraformational seal.

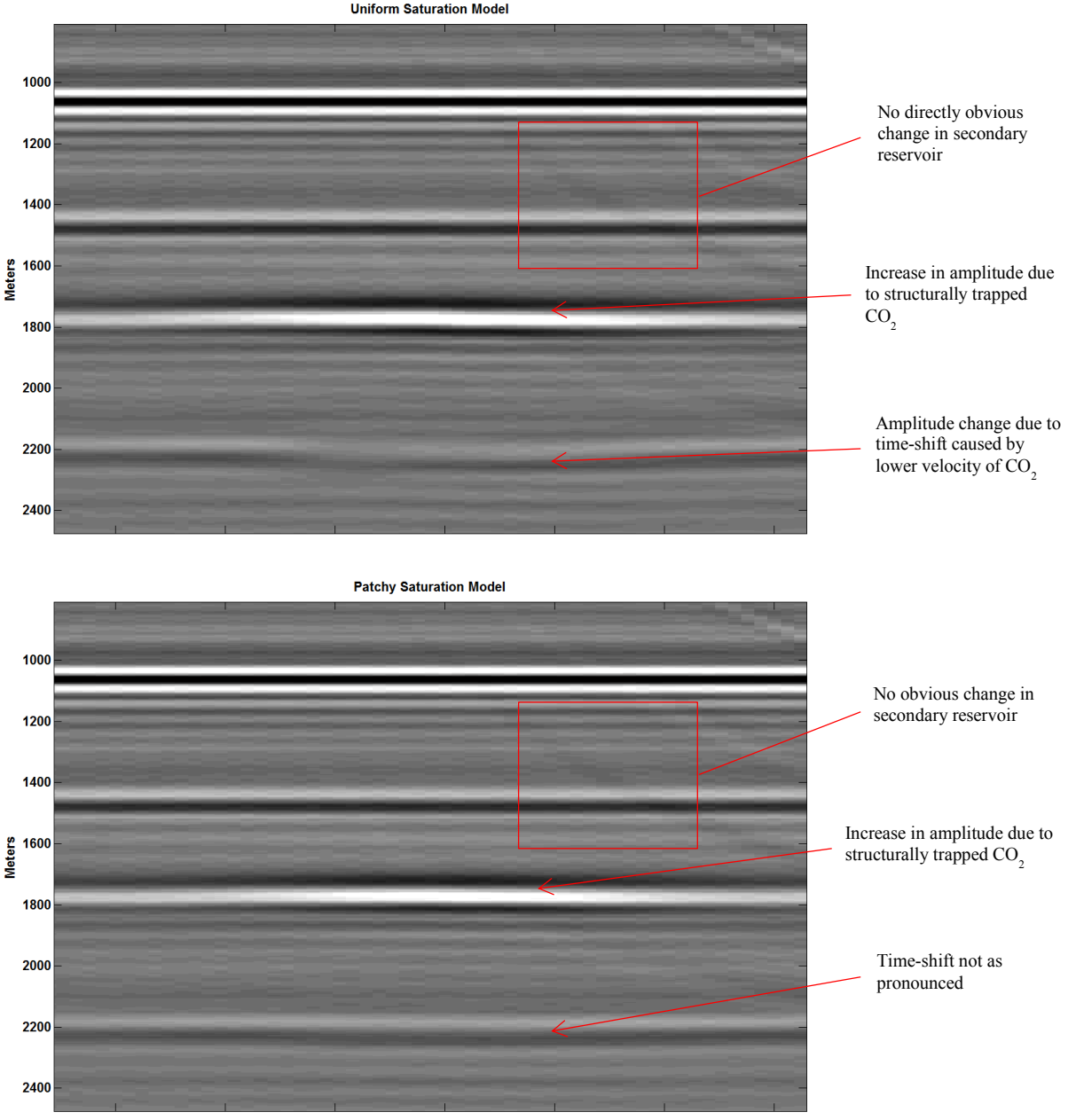

Fig. 6. Synthetic seismic modelling of the first instance of a loss of containment assuming a uniform (top) and patchy (bottom) velocity saturation model.

The time-lapse sections reveal details which are not easily observed in the monitor section alone. As illustrated below in Fig. 7, both sections clearly highlight the geometry of the structurally trapped CO_2, where the extent of the trapped CO_2 is estimated to span 750m. The amplitude is strongest at the centre and gradually becomes weaker, indicating that the saturation of CO_2 is highest at the crest of the structure and gradually decreases further out in both directions. This change is further highlighted when comparing the uniform and patchy models, showing weaker amplitude differences in the patchy model due to the gradational change in saturation, and hence in velocity, as opposed to the uniform velocity model.

The time-lapse section alone shows a weak amplitude anomaly in the secondary reservoir due to the migrating front. As can be expected, the uniform saturation model highlights this clearer due to the larger change in velocity at the lower saturations. This is evident at the depth of roughly 1450m, at the top of the intraformational seal. Although apparent, the very weak amplitude change using the patchy saturation model could be very difficult to interpret without knowledge of a loss of containment within the area. Furthermore, it is evident that the lateral extent of the migrating front is also much larger than the actual size of the migrating plume.

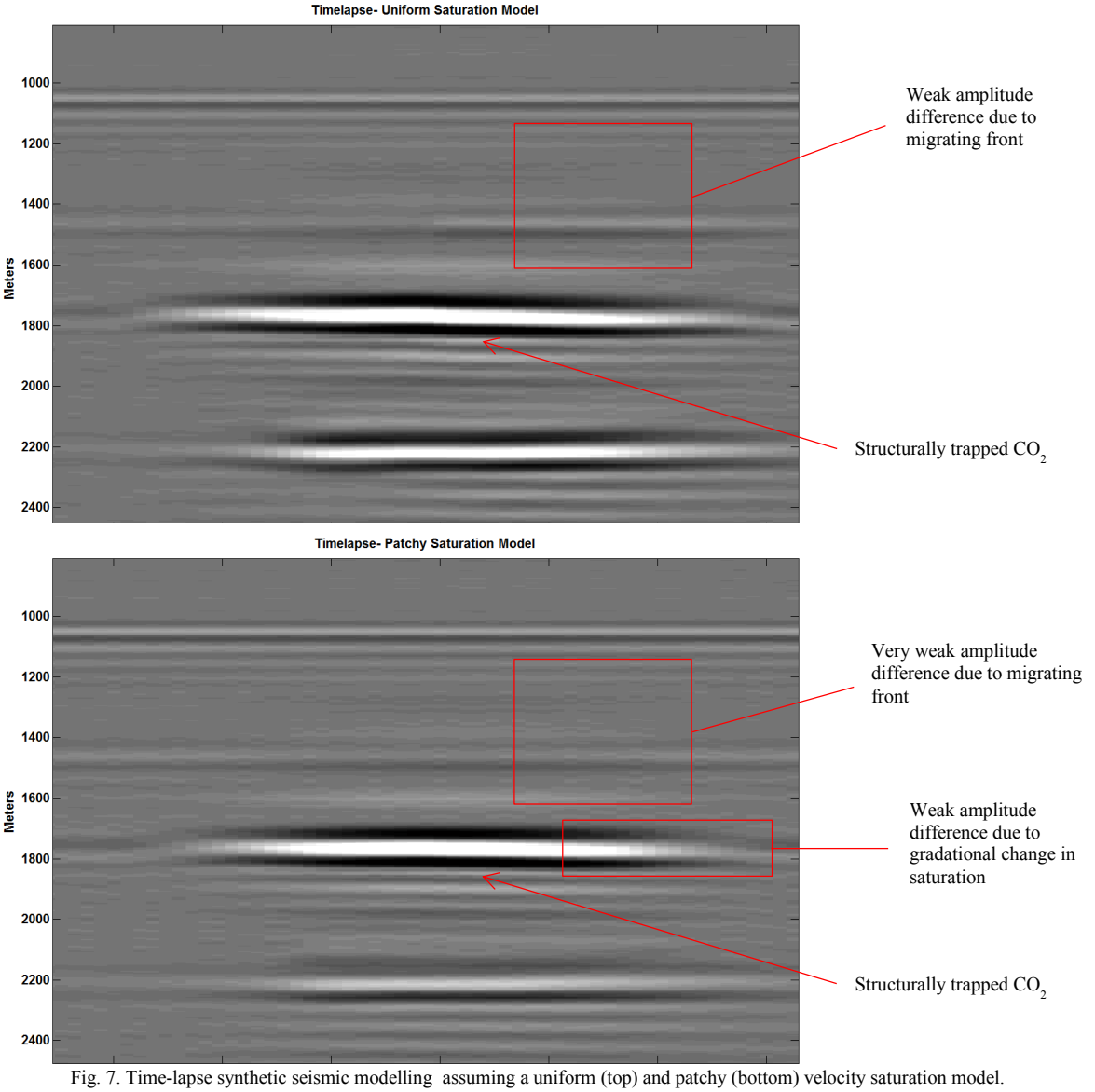

Fig. 7. Time-lapse synthetic seismic modelling assuming a uniform (top) and patchy (bottom) velocity saturation model.

6. Conclusions

In order to assess the feasibility for seismic monitoring of a migrating CO_2 front, we estimate the time-lapse signal over a theoretical, clean, homogeneous sandstone reservoir through the application of a three-stage model-driven workflow consisting of fluid-flow, rock physics and seismic forward modelling.

Once a migrating CO_2 front was simulated, the corresponding elastic properties were determined by calculating two saturation end-member models; uniform and modified-patchy saturation. This was done to understand the expect ranges which could be encountered when assessing the ability to detect a loss of containment. Analysis of the difference between the baseline velocity and the velocity of the migrating front clearly highlights the differences between the two models. It is shown that there is increased potential in detecting a loss of containment when assuming a uniform saturation model as opposed to patchy saturation, mainly due to the large change in velocity at the simulated concentrations of CO_2. At the migrating front, a change in velocity to the baseline is shown to be in the range of -200 to -50 m/s. If assuming that the velocity will follow a patchy saturation model, a change of only -50m/s can be expected. The calculated velocity of a migrating front showed minor, possibly detectable, changes in time-lapse signal when compared to the baseline model, for both velocity models.

From this a conservative conclusion could be made that seismic monitoring of a migrating front of CO_2 is feasible, however with great dependence on the saturation model used. In reality this might not be the case as the noise-free synthetic seismic show amplitude anomalies for an accumulation with a radius as small as 30m. This could be too optimistic, as the model was implemented at a cross-section across the known migration point. However, with this knowledge, feasibility studies conducted prior to injection could provide valuable information regarding potential migration hotspots which could assist in the design and construction of future surveys aiding in the detection of a loss of containment. Furthermore, the overall detectability of a migrating plume for the scenario chosen in this study is not a definite answer, as the saturations are controlled by the relative permeability and capillary pressure curves input into the simulation, where different curves, as well as varying injection rates, may predict a greater range of CO_2 saturations, and therefore, a greater change in elastic behaviour. This highlights the fact that the detectability of a migrating CO_2 front is a site specific issue which not only depends on the geophysical parameters of the seismic survey but also on the geological variations and spatial distribution in the reservoir. Assessing these site-specific variations, such as reservoir relative-permeability and heterogeneity, during initial storage-site assessment stages, could provide valuable information regarding the ability to detect CO_2 migration, aiding in the ability to detect a loss of containment, should one occur.

Acknowledgements

This work was sponsored by E.ON and ETP through SCCS. The authors would also like to thank Silke Bude at PGS and their colleagues at the University of Edinburgh, in particular, David Wright and Carlos da Costa Filho for their contribution to this study.

References

[1] EC, *Directive 2009/31/EC of the European Parliament and of the Council of 23 April 2009 on the Geological Storage of Carbon Dioxide.* European Commission, Brussels, 2009.
[2] Arts, R., et al., *Monitoring of CO_2 injected at Sleipner using time-lapse seismic data.* Energy, 2004. **29**(9): p. 1383-1392.
[3] Wilson, M. and M. Monea, *IEA GHG Weyburn CO_2 monitoring & storage project. Summary report 2000-2004.* 2004.
[4] Pearce, J., *Technology Status Review: Monitoring Technologies for the Geological Storage of CO_2.* 2005: DTI.
[5] White, J., *Computed seismic speeds and attenuation in rocks with partial gas saturation.* Geophysics, 1975. **40**(2): p. 224-232.
[6] Mavko, G. and T. Mukerji, *Bounds on low-frequency seismic velocities in partially saturated rocks.* Geophysics, 1998. **63**(3): p. 918-924.
[7] Cairns, G., et al., *Using time-lapse seismic monitoring to identify trapping mechanisms during CO_2 sequestration.* International Journal of Greenhouse Gas Control, 2012. **11**(0): p. 316-325.
[8] Class, H., et al., *A benchmark study on problems related to CO_2 storage in geologic formations.* Computational Geosciences, 2009. **13**(4): p. 409-434.
[9] Permedia, *BOS, Version 5.1.* Halliburton, Ottawat, Ontario, 2014.

[10] Bennion, D. and S. Bachu. *Dependence on temperature, pressure, and salinity of the IFT and relative permeability displacement characteristics of CO_2 injected in deep saline aquifers*. in *SPE Annual Technical Conference and Exhibition*. 2006.
[11] Bryant, S.L., S. Lakshminarasimhan, and G.A. Pope, *Buoyancy-dominated multiphase flow and its effect on geological sequestration of CO_2.* SPE Journal, 2008. **13**(04): p. 447-454.
[12] Silin, D., T.W. Patzek, and S.M. Benson, *A one-dimensional model of vertical gas plume migration through a heterogeneous porous medium.* International Journal of Greenhouse Gas Control, 2009. **3**(3): p. 300-310.
[13] Saadatpoor, E., S.L. Bryant, and K. Sepehrnoori, *New trapping mechanism in carbon sequestration.* Transport in Porous Media, 2010. **82**(1): p. 3-17.
[14] Smith, T.M., C.H. Sondergeld, and C.S. Rai, *Gassmann fluid substitutions: A tutorial.* Geophysics, 2003. **68**(2): p. 430-440.
[15] Dvorkin, J. and A. Nur, *Elasticity of high-porosity sandstones: Theory for two North Sea data sets.* Geophysics, 1996. **61**(5): p. 1363-1370.
[16] Avseth, P., T. Mukerji, and G. Mavko, *Quantitative seismic interpretation.* Quantitative Seismic Interpretation, by Per Avseth and Tapan Mukerji and Gary Mavko, pp. 376. ISBN 0521816017. Cambridge, UK: Cambridge University Press, March 2005., 2005. **1**.
[17] Berryman, J.G., *Origin of Gassmann's equations.* Geophysics, 1999. **64**(5): p. 1627-1629.
[18] Han, D.-h. and M.L. Batzle, *Gassmann's equation and fluid-saturation effects on seismic velocities.* Geophysics, 2004. **69**(2): p. 398-405.
[19] Adam, L., M. Batzle, and I. Brevik, *Gassmann's fluid substitution and shear modulus variability in carbonates at laboratory seismic and ultrasonic frequencies.* Geophysics, 2006. **71**(6): p. F173-F183.